Article

Cell Reports

The Coding Regions of Germline mRNAs Confer Sensitivity to Argonaute Regulation in *C. elegans*

Graphical Abstract

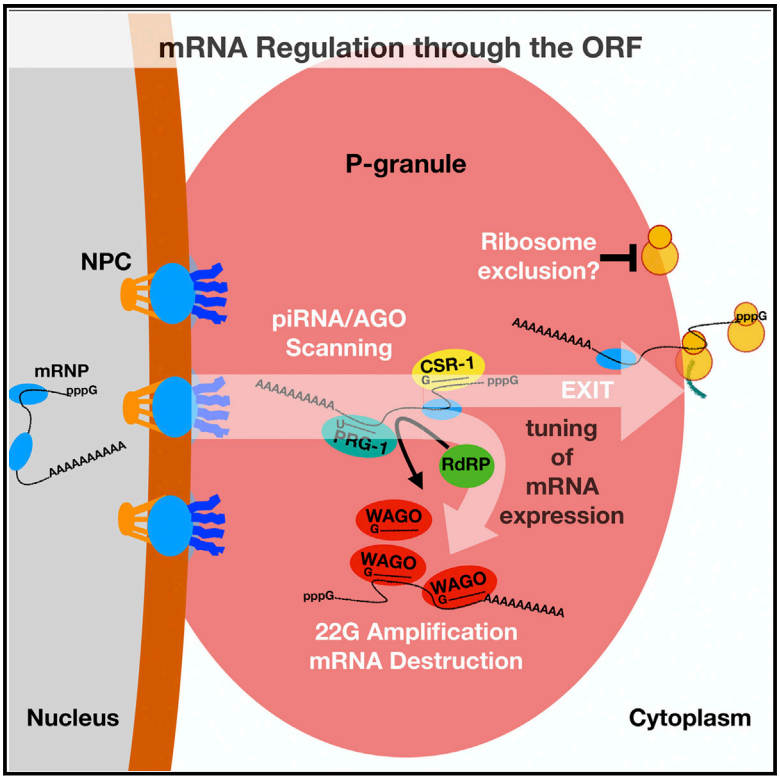

Authors

Meetu Seth, Masaki Shirayama, Wen Tang, ..., Heng-Chi Lee, Zhiping Weng, Craig C. Mello

Correspondence

craig.mello@umassmed.edu

In Brief

Some *C. elegans* transgenes resist piRNA silencing. Seth et al. map resistance to endogenous sequences within transgenes and show that artificially increasing piRNA targeting can incrementally reduce expression without silencing. Their findings identify coding regions as part of a rich piRNA regulatory landscape within perinuclear nuage.

Highlights

- *C. elegans* germline mRNAs differ in sensitivity to piRNA targeting
- piRNA targeting of coding regions provides incremental control of gene expression
- Piwi Argonaute surveillance occurs upstream of nonsense-mediated decay
- Model, piRNAs scan mRNAs within perinuclear nuage prior to translation initiation

Seth et al., 2018, Cell Reports *22*, 2254–2264
February 27, 2018
https://doi.org/10.1016/j.celrep.2018.02.009

CellPress

OPEN ACCESS
CellPress

Cell Reports
Article

The Coding Regions of Germline mRNAs Confer Sensitivity to Argonaute Regulation in *C. elegans*

Meetu Seth,[1,2,4] Masaki Shirayama,[1,2] Wen Tang,[1] En-Zhi Shen,[1] Shikui Tu,[3,5] Heng-Chi Lee,[1,6] Zhiping Weng,[3] and Craig C. Mello[1,2,7,*]

[1]RNA Therapeutics Institute, UMass Medical School, 368 Plantation Street, Worcester, MA 01605, USA
[2]Howard Hughes Medical Institute
[3]Program in Bioinformatics and Integrative Biology, UMass Medical School, 368 Plantation Street, Worcester, MA 01605, USA
[4]Present address: Intellia Therapeutics, 40 Erie Street, Cambridge, MA 02139, USA
[5]Present address: Center for Cognitive Machines and Computational Health and Department of Computer Science and Engineering, School of Electronic Information and Electrical Engineering, Shanghai Jiao Tong University, Shanghai, China
[6]Present address: University of Chicago, 920E 58th Street, Chicago, IL 60637, USA
[7]Lead Contact
*Correspondence: craig.mello@umassmed.edu
https://doi.org/10.1016/j.celrep.2018.02.009

SUMMARY

Protein-coding genes undergo a wide array of regulatory interactions with factors that engage non-coding regions. Open reading frames (ORFs), in contrast, are thought to be constrained by coding function, precluding a major role in gene regulation. Here, we explore Piwi-interacting (pi)RNA-mediated transgene silencing in *C. elegans* and show that marked differences in the sensitivity to piRNA silencing map to the endogenous sequences within transgene ORFs. Artificially increasing piRNA targeting within the ORF of a resistant transgene can lead to a partial yet stable reduction in expression, revealing that piRNAs not only silence but can also "tune" gene expression. Our findings support a model that involves a temporal element to mRNA regulation by germline Argonautes, likely prior to translation, and suggest that piRNAs afford incremental control of germline mRNA expression by targeting the body of the mRNA, including the coding region.

INTRODUCTION

Cells utilize RNA-guided search mechanisms to find and regulate genetic information. Mechanisms of this type include the Argonaute-mediated response termed RNA interference (RNAi) (Fire et al., 1998) and the independently evolved bacterial antiviral CRISPR/CAS system (Bhaya et al., 2011; Marraffini and Sontheimer, 2010). In addition to cellular defense, organisms employ RNA-guided mechanisms to regulate endogenous gene expression. For example, the microRNA (miRNA) Argonaute-mediated pathway employs cellular transcription to produce RNA guides that carry out mRNA regulation (Ghildiyal and Zamore, 2009; Lee et al., 1993; Wightman et al., 1993). The miRNA Argonaute system tolerates mismatched pairing between miRNA and target mRNA, allowing the few hundred miRNAs typically present in most animal genomes to regulate a substantial fraction of mRNAs (Grimson et al., 2007; Helwak et al., 2013; Lewis et al., 2005).

Among the most enigmatic of small RNA pathways is the Piwi-interacting (pi)RNA pathway (Aravin et al., 2006; Girard et al., 2006; Grivna et al., 2006; Lau et al., 2006; Ruby et al., 2006). piRNAs engage Argonaute proteins related to the *Drosophila* Piwi (P element-induced, wimpy testes) protein (Cox et al., 1998; Lin and Spradling, 1997). piRNAs derive from precursors that are transcribed by RNA polymerase II, and their production requires nucleolytic processing at their 5′ and 3′ ends (Ipsaro et al., 2012; Izumi et al., 2016; Nishimasu et al., 2012; Tang et al., 2016). While some piRNAs target transposons, many have no perfectly matched mRNA targets (Bagijn et al., 2012; Lee et al., 2012; Vourekas et al., 2012).

Studies on mouse Piwi proteins suggest that they may regulate endogenous genes. For example, Goh et al. (2015) provide evidence for piRNA-directed targeting of meiotically expressed protein-coding genes in the mouse testes. Another study suggests that piRNAs may direct massive mRNA elimination in elongating spermatids (Gou et al., 2014). In *C. elegans*, piRNAs can induce stable transgenerational silencing of foreign genes and are thought to do so while allowing miRNA-like, partially mismatched base-pairing (Ashe et al., 2012; Bagijn et al., 2012; Lee et al., 2012; Shirayama et al., 2012). Upon target binding, the Piwi-related protein (PRG-1) recruits RNA-dependent RNA polymerase (RdRP) to produce secondary small RNAs (22G-RNAs) that load onto members of an expanded group of worm-specific Argonautes (WAGOs). WAGOs, in turn, maintain and propagate a form of epigenetic silencing termed RNA-induced epigenetic silencing (RNAe) (Shirayama et al., 2012).

A curious feature of RNAe is that WAGOs target the foreign portions of a silenced transgene (e.g., the *gfp* open reading frame [ORF]) but not the endogenous sequences fused to *gfp* within the same transgene (Shirayama et al., 2012). How these endogenous sequences are protected from WAGO targeting remains unclear, but a recent study suggests that it is not simply because piRNAs fail to target sequences that resist RNAe (Shen et al., 2018). Indeed, Shen et al. (2018) revealed that piRNAs bind with miRNA-like seed and supplementary pairing

but do so within the ORFs as well as the UTRs of essentially all germline mRNAs.

Interestingly, a third germline Argonaute system, the CSR-1 pathway, engages small RNAs produced by RdRP that are antisense to most germline mRNAs (Claycomb et al., 2009). CSR-1 targeting correlates with resistance to WAGO silencing. Several lines of evidence suggest that CSR-1 provides a protective memory of self-gene expression and that this protection is necessary for germline mRNAs to avoid piRNA silencing. First, as noted above, the diversity and relaxed-targeting rules of piRNAs mean that germline mRNAs cannot entirely avoid piRNA targeting. Second, essentially all expressed germline mRNAs are targeted by CSR-1, and with very few exceptions (Gerson-Gurwitz et al., 2016), their expression is not increased in *csr-1* mutants. Thus, CSR-1 does not silence the vast majority of its targets. Third, when transgenes are introduced at single copy, in defined chromosomal locations, only those transgenes containing foreign sequences (e.g., *gfp*) undergo silencing (Shirayama et al., 2012). Fourth, some *gfp* transgenes escape piRNA-induced silencing and also resist WAGO silencing. This resistance correlates with targeting of the *gfp* sequences by CSR-1 22G-RNAs (Seth et al., 2013). Fifth, when CSR-1 targets *gfp* sequences, the transgene can transactivate silenced *gfp* transgenes (Shirayama et al., 2012), and its ability to transactivate depends on CSR-1 activity (Seth et al., 2013). Moreover, artificially tethering CSR-1 to a target mRNA can drive the activation of a normally silent transgene (Wedeles et al., 2013). Finally, when CSR-1 activity is depleted, piRNA targeting increases on germline mRNAs transcriptome wide (Shen et al., 2018).

Thus, numerous lines of evidence suggest that CSR-1 targeting provides a memory of self-gene expression that is necessary to protect mRNAs from piRNA-mediated silencing in *C. elegans*. The term RNA activation, RNAa, describes the process by which a CSR-1-targeted transgene can activate a silent transgene that shares sequence identity (Seth et al., 2013). Interestingly, both CSR-1 and WAGO Argonautes and their associated small RNAs are transmitted to offspring in both the sperm and the egg, providing a mechanism for the inheritance for these "memories" of parental gene-expression states (Conine et al., 2010, 2013).

In *C. elegans*, both CSR-1 and PRG-1, as well as members of the WAGO Argonaute family, reside within perinuclear germline nuage structures termed P granules (Batista et al., 2008; Claycomb et al., 2009; Gu et al., 2009). CSR-1 is required for the perinuclear localization of the P granules, suggesting that the targeting of nascent mRNAs by CSR-1 may induce the recruitment (or condensation) of P granules at the nuclear periphery (Claycomb et al., 2009; Updike and Strome, 2009). In wild-type animals, P granules surround nuclei in close apposition to nuclear pores, and mRNAs are thought to transit through P granules after nuclear exit (Schisa et al., 2001; Sheth et al., 2010). These observations have prompted the hypothesis that P granules represent a ribosome-free zone where nascent mRNAs may undergo regulation in germ cells prior to the onset of translation (Sheth et al., 2010; Updike and Strome, 2010; Updike et al., 2011).

Here, we explore marked differences in the sensitivity of two transgenes to piRNA-induced silencing. We map the sequences that confer these differences to the ORFs of the endogenous sequences in these transgenes. We show that resistance to silencing does not depend (solely) on CSR-1 targeting. We show that piRNA surveillance occurs even on transcripts that undergo nonsense-mediated decay, a co-translational surveillance mechanism that destroys transcripts containing premature stop codons (Baker and Parker, 2004; Chang et al., 2007). Our findings support a model that involves regulation by germline Argonautes at a step prior to mRNA translation and suggest that regulation occurs within a context of other, as yet unknown regulators that also engage the coding region of the mRNA to afford incremental control of germline mRNA expression.

RESULTS

In the course of our investigation of transgene interactions, we identified numerous *gfp* fusions that were able to transactivate silent *gfp* transgenes. These activating transgenes included *oma-1::gfp*, *wrm-1::gfp*, *oma-2::gfp*, and *pie-1::gfp* (Shirayama et al., 2012). A search for features of these transgenes or their corresponding endogenous genes that might explain their properties did not reveal any obvious correlations. The transgenes themselves were not more abundantly expressed nor were the corresponding endogenous genes expressed at higher levels. Moreover, as compared to the endogenous regions in transgenes prone to silencing, the endogenous sequences within RNAa-competent transgenes were neither targeted by more CSR-1 22G-RNAs nor by fewer piRNAs (Figure S1; Shen et al., 2018). These observations suggest that the anti-silencing features of RNAa transgenes do not result from bypassing or overwhelming the RNAe system. Instead, we speculated that they somehow promote the spread of CSR-1 targeting from the endogenous sequences to the *gfp* sequences in the transgene (Seth et al., 2013; Shirayama et al., 2012).

Balanced Silencing and Activating Signals

To explore the question of why transgenes differ in sensitivity to silencing, we decided to make a detailed investigation of the RNAa transgene *oma-1::gfp.* During this analysis, we found that multiple independently isolated *oma-1::gfp* transgenes could reproducibly transactivate the silent, RNAe, transgenes *gfp::cdk-1* and *gfp::csr-1* (green arrows, Figure 1A). Surprisingly, however, we identified occasional pairings in which RNAa failed to occur (red arrows, Figure 1A), and the transgenes instead adopted a stable balanced state, with the *oma-1::gfp* transgene expressed and the RNAe transgenes silent (Figure 1B). Consistent with the idea that an RNAe-dependent mechanism maintains silencing in this balanced state, we found that the introduction of a mutation in *rde-3(ne3370)*, a gene required for RNAe (Shirayama et al., 2012), robustly reactivated GFP::CSR-1 expression.

PRG-1 activity was previously shown to be required to initiate RNAe or to re-silence a transgene activated by RNAa but not to maintain RNAe once established (Seth et al., 2013; Shirayama et al., 2012). We therefore asked whether *prg-1* activity is required to maintain silencing in the balanced *oma-1::gfp gfp::csr-1* double transgenic strain. We found that while, as expected, the *gfp::csr-1* single transgenic strain remained silenced in *prg-1* mutants ($n > 20$), the GFP::CSR-1 protein became robustly expressed in 100% of the *prg-1(tm872)* homozygous strains that also contained *oma-1::gfp* ($n = 60$; Figure 1C). Thus, *oma-1::gfp*

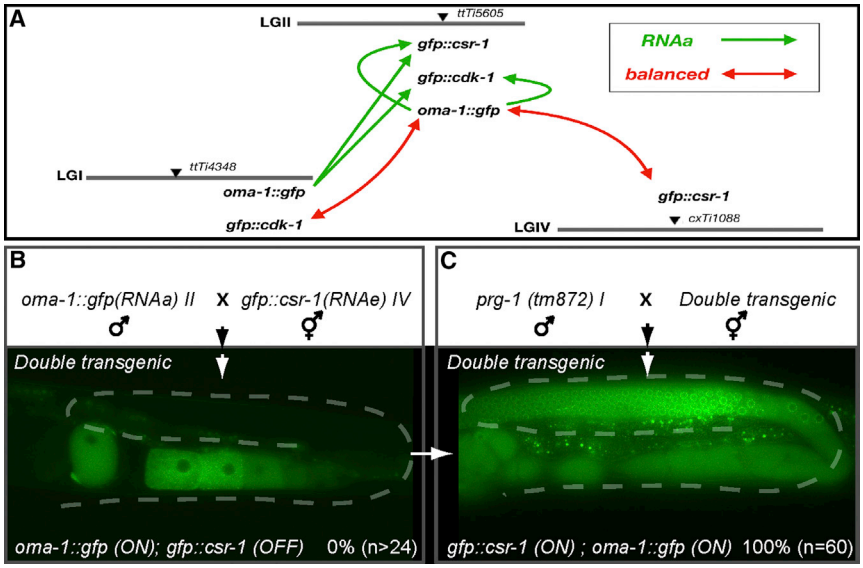

Figure 1. Balanced Silencing and Activation Signals

(A) Transgene insertion at different chromosomal locations by MOSCI (see Supplemental Experimental Procedures) and summarizing the interactions between transgenes inserted at these locations.

(B and C) Epifluorescence image of representative germlines (outlined with dashes) within transgenic strains (as indicated). The cytoplasmic fluorescence signal is OMA-1::GFP; the P granule signal is GFP::CSR-1. The percentages indicate the number of animals that exhibited the expression of GFP::CSR-1 in the wild-type and *prg-1* (tm872) mutant after at least two generations of maintenance of the double transgenic strains.

See also Figure S1.

can transactivate *gfp::csr-1* inserted at *cxTi10882* on LGIV but only when *prg-1* activity is absent. These findings indicate that, although *oma-1::gfp* exerts a positive influence on the *gfp::csr-1* transgene located at *cxTi10882*, it is not sufficient to overcome the combined activities of the WAGO-silencing machinery and continued piRNA/PRG-1 targeting. Thus, in addition to initiating RNAe as previously shown (Shirayama et al., 2012), these findings show that PRG-1 can also function in some instances to maintain and reinforce silencing.

Transgenes Differ in Their Responses to piRNA Targeting

In the above experiments, differences in the chromosomal insertion sites were correlated with differences in the interactions between transgenes. While it would be very interesting to understand these chromosomal influences in more detail, we decided to first attempt to address the more tractable question of why transgenes inserted at the same location respond differently to piRNA targeting. To address this question, we chose to compare the silencing-resistant *oma-1::gfp* and the silencing-prone *gfp::cdk-1* transgenes. We asked how these two transgenes responded to increased piRNA targeting. Using CRISPR-mediated homologous recombination (Dickinson and Goldstein, 2016; Friedland et al., 2013; Jinek et al., 2013; Kim et al., 2014; see Supplemental Experimental Procedures), we replaced the most abundantly expressed piRNA, *21ux-1* (Gu et al., 2012), with a sequence antisense to *gfp* (Figure 2A) and then crossed the *21ux-1(anti-gfp)* worms to animals expressing *cdk-1::gfp*. As expected, the *cdk-1::gfp* transgene was rapidly silenced after crossing to *21ux-1(anti-gfp)* worms (n > 20) (Figure S2A), indicating that the engineered piRNA is expressed and functional. Small RNA sequencing also confirmed robust expression of the *21ux-1(anti-gfp)* piRNA. Nevertheless, the *21ux-1(anti-gfp)* piRNA failed to silence the *oma-1::gfp* transgene, even when *21ux-1(anti-gfp)* was homozygous in the strain (n > 20) (Figure S2B). Strikingly, however, when we crossed these strains together to generate a double transgenic *cdk-1::gfp; oma-1::gfp* strain homozygous for *21ux-1(anti-gfp)*, rather than observing transactivation of *cdk-1::gfp*, we observed silencing of *oma-1::gfp* (n > 20) (Figure S2C). Thus, the addition of the *21ux-1(anti-gfp)* piRNA abolishes the ability of *oma-1::gfp* to transactivate a silent transgene and renders *oma-1::gfp* sensitive to transitive silencing.

We next used high-throughput sequencing to ask how the addition of *21ux-1(anti-gfp)* influenced 22G-RNA induction on the silencing-resistant *oma-1::gfp* and on the expressed but more silencing-prone *cdk-1::gfp* transgenes. Strikingly, on *cdk-1::gfp* we found that 22G-RNA induction occurred both locally, i.e., near the *21ux-1(anti-gfp)* target site, and at numerous regions distributed along the *gfp* portion of the transgene. The *21ux-1(anti-gfp)* target site was correlated with three major peaks of 22G-RNA biogenesis initiating at C residues at both ends and the middle of the target mRNA region (Figures 2D and 2E). By contrast, in the resistant *oma-1::gfp* transgenics, we observed a dramatically muted 22G-RNA response with only a single abundant 22G-RNA species positioned near the 3′ end of the *21ux-1(anti-gfp)* piRNA target region (Figures 2B and 2C). This finding suggests that some property of the *oma-1::gfp* mRNA prevents the accumulation and spread of 22G-RNA production along the length of the transgene.

Although immunofluorescence analysis indicated that *oma-1::gfp* remained expressed, we also monitored the levels of the corresponding mRNA and protein products. As expected, the *cdk-1::gfp* transgene was strongly silenced both at the mRNA and protein levels (Figures 2F and 2G). However, though still visible by microscopy, the mRNA and protein levels of *oma-1::gfp* signal were clearly reduced (Figures 2F and 2G), suggesting that the additional piRNA can partially reduce *oma-1::gfp* expression without inducing RNAe.

Increasing piRNA Targeting Can Drive PRG-1-Dependent Silencing

The above findings prompted us to ask whether engineering additional piRNAs that target *oma-1::gfp* could ultimately render the transgene sensitive to piRNA-induced silencing. Using

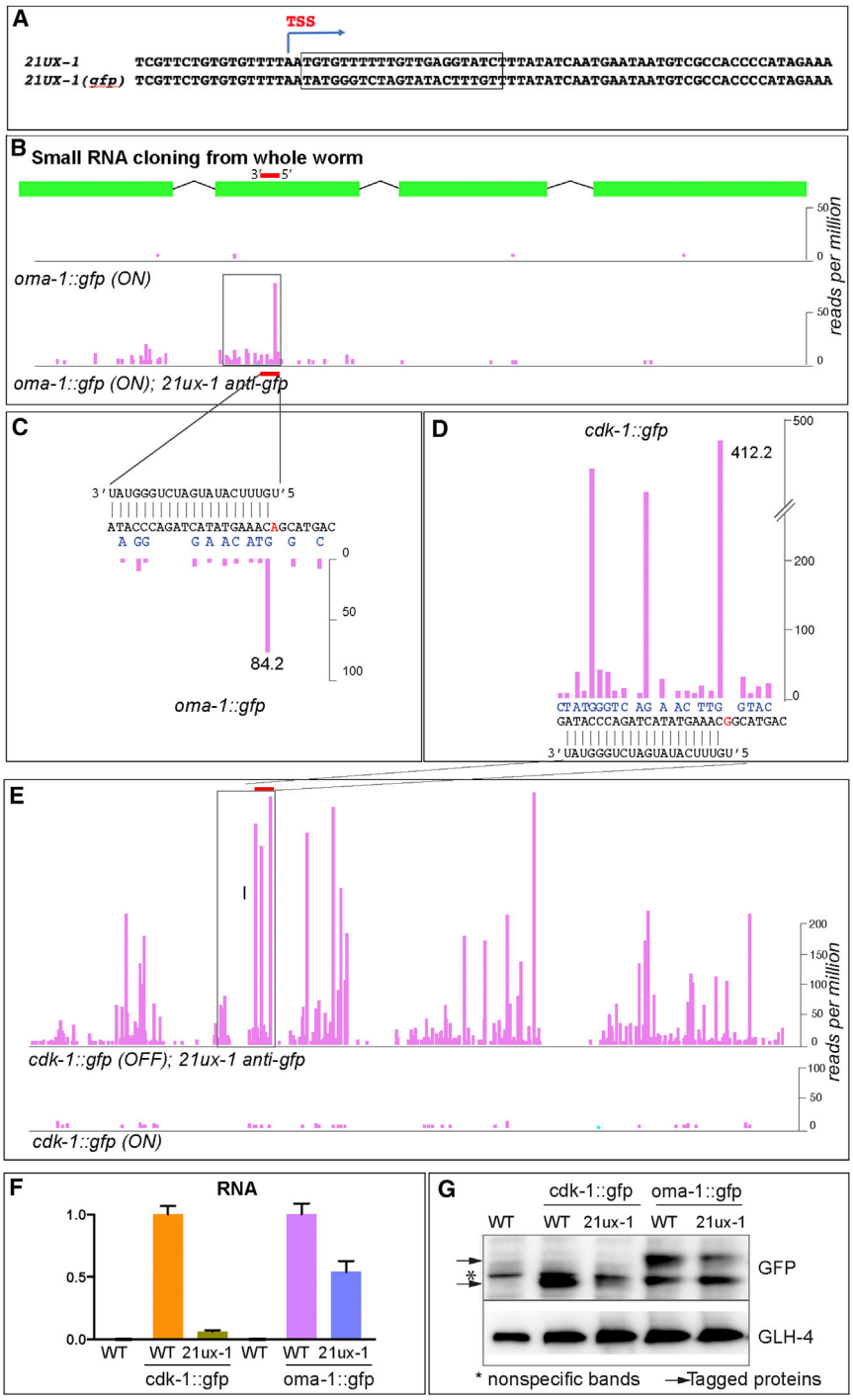

Figure 2. Transgenes Differ in Their Responses to piRNA Targeting

(A) Schematic representing the replacement of 21ux-1 with an anti-gfp sequence.

(B–E) Schematics showing plots of small RNA species induced along gfp in *oma-1::gfp* (B) and in *cdk-1::gfp* (E) transgenic animals. Each bar indicates the 5′ end of a small RNA species, and the height indicates abundance in reads per million. In (B), the upper plot shows the very low density of 22G-RNAs detected in *oma-1::gfp* wild-type transgenic animals, while the lower plot shows locally induced 22G-RNAs in *21ux-1(anti-gfp)* animals. In (C) and (D), *21ux-1(anti-gfp)* is shown base-paired to the *gfp* sequence, and induced small RNAs are plotted above each nucleotide in *oma-1::gfp* (C) and in *cdk-1::gfp* (D) *21ux-1(anti-gfp)* transgenic animals. In (E), 22G-RNA levels are shown in *cdk-1::gfp* transgenic animals that express *21ux-1(anti-gfp)* (upper plot) and in wild-type transgenic animals (lower plot).

(F) qRT-PCR analysis of *cdk-1::gfp*-RNA and *oma-1::gfp*-RNA from total RNA prepared from different transgenic strains (as indicated). Error bars represent the standard deviation for three replicates in one experiment.

(G) Western blot analysis of GFP protein expression in wild-type and transgenic strains (as indicated). As a loading control, the blot was stripped and re-probed for the germline specific GLH-4 protein.

See also Figures S1 and S2.

CRISPR, we replaced two adjacent abundantly expressed piRNAs (*21ur-11498* and *21ur-2675*) (Figure 3A) with sequences antisense to the *oma-1* mRNA. This double piRNA mutant strain also failed to silence *oma-1::gfp* (Figure S3A). However, when all three engineered piRNAs (both *anti-oma-1* piRNAs and the *21ux-1(anti-gfp)* piRNA) were present together in the same strain, we finally observed *oma-1::gfp* silencing (Figure S3B).

As expected, we found that the addition of the new piRNAs was correlated with the accumulation of 22G-RNAs near the target sites, especially the 21ux-1(anti-gfp) target site (Figures 3B–3D). As expected, the *oma-1::gfp* transgene was strongly silenced both at the mRNA and protein levels (Figures 3E and 3F). Interestingly, crossing the *prg-1 (tm872)* mutation into this silenced strain reactivated *oma-1::gfp* (n > 20). Thus, silencing of *oma-1::gfp* via these engineered piRNAs requires continuous PRG-1 targeting.

Properties Intrinsic to the *oma-1* Coding Sequences Confer Resistance to Silencing

We next wished to explore which features render the *oma-1::gfp* transgene more resistant to silencing than the *cdk-1::gfp* transgene. We therefore performed a number of swaps of sequence domains from these genes and monitored how these changes affected expression when re-inserted within exactly the same chromosomal location. We found that neither the promoter, 3′UTR, nor introns of *oma-1::gfp* were required for its RNAa properties (Figures 4A and 4B). An *oma-1::gfp* fusion driven by the *cdk-1* promoter and 3′ UTR was resistant to

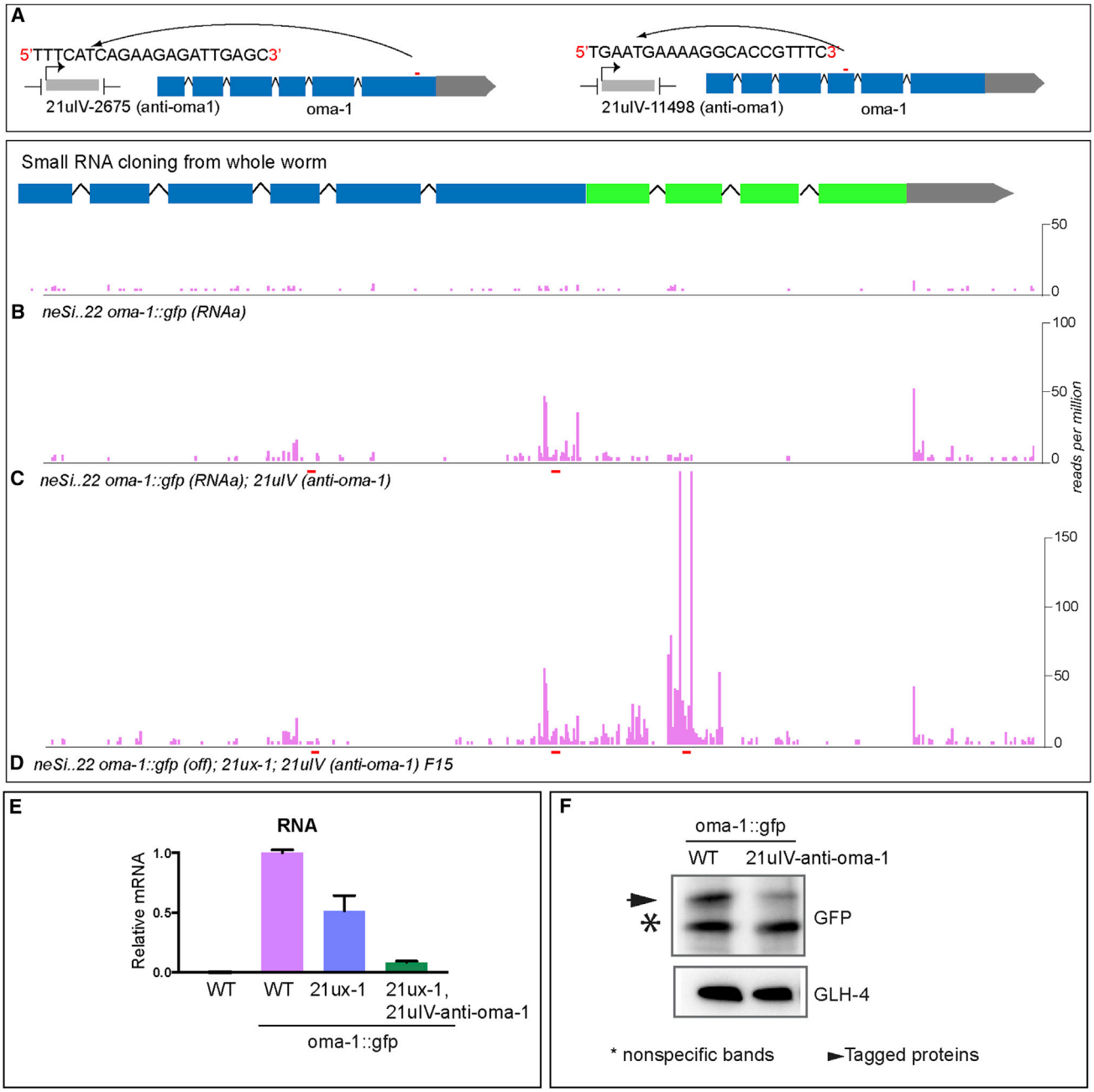

Figure 3. Increasing piRNA Targeting Induces *oma-1::gfp* to Silence

(A) Schematic representing the replacement of 21U-2675 IV and 21U-11498 IV with anti-oma-1 sequence.

(B–D) Schematics showing plots of small RNA species induced along the entire *oma-1::gfp* transgene in (B) wildtype, (C) *21uIV-11498(anti-oma1)* and *21uIV-2675(anti-oma1)* animals, and (D) *21uIV-11498(anti-oma1)*, *21uIV-2675(anti-oma1)*, and *21ux-1(anti-gfp)* animals. In the browser schematic, *oma-1* sequences are blue, fused to green gfp sequences. The positions of each artificial piRNA are indicated by red dash marks beneath the small RNA graphs. The 5′ ends of small RNA reads are plotted, and the height indicates abundance in reads per million.

(E) qRT-PCR analysis of wild-type (WT) and *oma-1::gfp*-RNA from total RNA prepared from different transgenic strains (as indicated). Error bars represent the standard deviation for three replicates in one experiment.

(F) Western blot analysis of GFP protein expression in wild-type and transgenic strains (as indicated). As a loading control, the blot was stripped and re-probed for the germline-specific GLH-4 protein.

See also Figure S3.

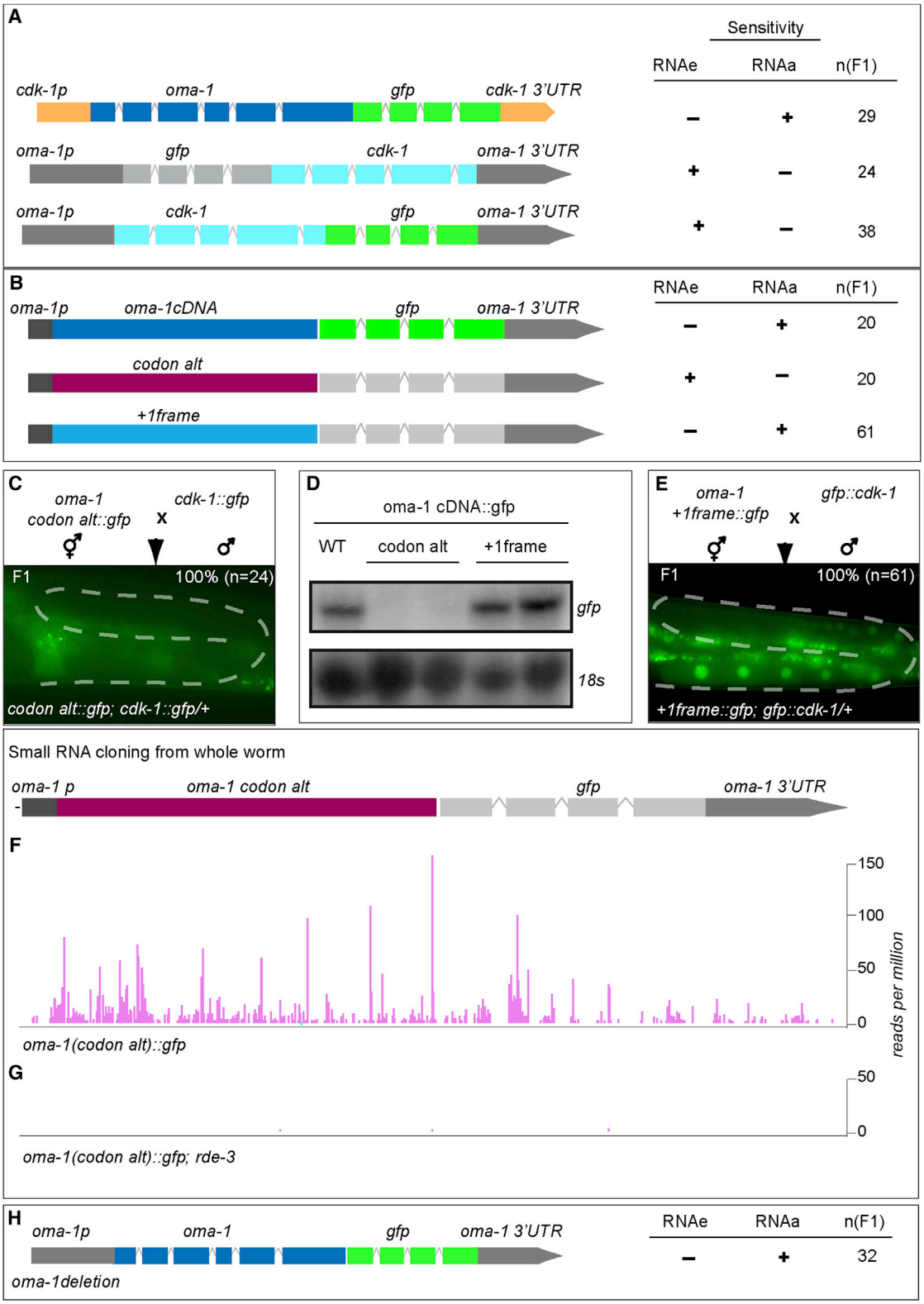

Figure 4. Properties Intrinsic to the *oma-1* Coding Sequences Confer Resistance to Silencing

(A and B) Promoters, UTRs, and introns do not determine transgene sensitivity/resistance to silencing. Schematics indicating the exon-intron structure of fusion genes analyzed are displayed alongside tabulations of their respective RNAe and RNAa activities. Transgenes were scored as (+) if they could act in *trans* to

(legend continued on next page)

silencing and retained the ability to transactivate a silent *gfp* transgene (Figure 4A). Conversely, *cdk-1::gfp* controlled by the *oma-1* promoter and 3′ UTR remained prone to silencing (Figure 4A).

The above findings suggest that the sequences comprising the coding region of *oma-1* confer resistance to silencing. To more directly test this idea we decided to re-code the OMA-1 protein to maximize nucleotide differences while maintaining the amino acid sequence of OMA-1. Upon introduction, we found that all of the (n > 20) independently generated codon-altered *oma-1:gfp* transgenes analyzed were silent, with no detectable GFP fluorescence or mRNA expression (Figures 4B and 4D). Moreover, we found that a silent codon-altered *oma-1::gfp* transgene was able to act in *trans* to silence an expressed allele of *cdk-1::gfp* (Figure 4C). Consistent with an RNAe mechanism, we found that introducing a mutation in *rde-3* resulted in the activation of the silent re-coded *oma-1::gfp* allele (n > 20) and, as expected, also caused the loss of 22G-RNAs targeting the transgene (Figures 4F and 4G). Instead of exhibiting 22G-RNA accumulation only within the *gfp* portion of the transgene, as is normally seen in RNAe-silenced transgenes (e.g., *gfp::cdk-1*) (Shirayama et al., 2012), we observed RDE-3-dependent 22G-RNA accumulation throughout the codon-altered region of *oma-1* in this strain (Figures 4F and 4G). Thus, the RNAe machinery appears to target both the *oma-1* and *gfp* sequences equally to drive silencing of this transgene.

A possible explanation for the above findings was that altering the codons of *oma-1* rendered the mRNA less optimal for translation (Presnyak et al., 2015), perhaps predisposing it to silencing. We therefore generated a second transgene in which we shifted the *oma-1* ORF by removing one nucleotide after the ATG, replacing 11 stop codons with sense codons, and adding a nucleotide just before the *gfp* sequence to maintain the *gfp* reading frame. This +1-frame transgene encodes a novel protein with non-optimal codons but with a nucleotide sequence nearly identical to *oma-1*. Although the +1-frame transgene did not produce a visible GFP signal, the level of mRNA was similar to that produced by the unaltered *oma-1cDNA::gfp* transgene (Figure 4D). Moreover, we found that this +1-frame transgene was able to transactivate a silent *gfp* transgene (Figure 4E). Taken together, these findings suggest that the nucleotide sequence of the *oma-1* coding region, and not, for example, the additional production of OMA-1 protein, confers resistance to RNAe-mediated silencing.

A plausible model for how *oma-1::gfp* acquires RNAa activity is that pre-existing CSR-1 22G-RNAs (templated from the endogenous *oma-1* mRNA) spread to the nearby *gfp* sequences via local recruitment of RdRP to the *oma-1* region of the *oma-1::gfp* mRNA. Altering the codons of *oma-1* could thus abolish CSR-1-dependent protection of the *oma-1* region, essentially making the entire gene into a "foreign" transgene, and thus prone to piRNA targeting. To test this idea, we made a strain that completely lacks all genomic sequences complementary to the *oma-1::gfp* transgene. We used genome editing to remove the entire *oma-1* gene including its 3′ UTR. Although small regions of *oma-2* have nucleotide sequences similar to *oma-1*, none of these regions produces CSR-1 22G-RNAs that match *oma-1.* Deletion of endogenous *oma-1* should thus completely remove all portions of the transcriptome that could provide transitive CSR-1 22G-RNAs complementary to the *oma-1::gfp* transgene. Surprisingly, upon *de novo* introduction into this strain, we found that the *oma-1::gfp* transgene (n = 2) continued to exhibit robust RNAa activity in crosses with a silent *gfp::cdk-1* strain that also contains the complete genomic deletion of *oma-1* (Figure 4H). These findings suggest that the resistance of *oma-1::gfp* to RNAe reflects intrinsic properties of the transgene coding sequences.

Premature Nonsense Mutations Do Not Prevent RNAa and RNAe

In many eukaryotes, mRNAs containing a premature stop codon undergo degradation via a conserved pathway known as nonsense-mediated decay (NMD) (Baker and Parker, 2004; Chang et al., 2007). Since both RNAa and RNAe utilize mRNAs as templates for secondary sRNA production, we reasoned that NMD silencing could suppress template levels necessary for these Argonaute-mediated pathways. Alternatively, since many endogenous RNAe targets are pseudo genes that contain numerous stop codons (Gu et al., 2009), NMD might act to predispose mRNAs to silencing.

To explore the relationship between NMD and Argonaute pathways, we generated transgenes containing premature stop codons and assayed their ability to respond to RNAa and RNAe surveillance mechanisms. To explore the consequences of premature stop codons on an RNAe-inducing transgene, we constructed the silencing-prone *gfp::cdk-1* transgene with a stop codon in the second exon of gfp (n > 3) (Figure 5A). We first confirmed that this transgene was sensitive to NMD. As expected, we found that expression of *gfp* (Y_{74}stop)*::cdk-1* was not detected when introduced into wild-type animals, and expression was not restored in *rde-3* mutants (data not shown). When crossed to an expressed *cdk-1::gfp* transgene, we found that that all of the

silence (RNAe) or activate (RNAa) another transgene. In (A), the (s) indicates that the *cdk-1::gfp* transgene was expressed but was sensitive to RNAe. For each transgene type, 100% of the (n) F1 cross progeny analyzed exhibited the same sensitivity.
(C–G) The body of the mRNA, but not its coding potential, determines sensitivity/resistance to silencing. In (C) and (E), schematics of genetic crosses are shown above representative epifluorescence images of F1 progeny (percentages indicate the number of F1 animals that exhibited the expression pattern shown). In (C), codon-altered *oma-1::gfp* is silent and induces the silencing of *cdk-1::gfp* (absence of nuclear GFP signal).
(D) Northern blot analysis of *gfp* mRNA expression in animals transgenic for *gfp* fused to oma-1 cDNA sequences with un-altered codons (WT), with maximally altered codons (codon alt), and with a frameshifted and stop-codon-corrected (+1frame) oma-1 sequence.
(E) Frameshifted oma-1::gfp induces the transactivation of a silent *gfp::cdk-1* (nuclear GFP signal).
(F and G) *oma-1(codon alt)::gfp* is silenced by RNAe. Plots show 22G-RNA levels in wild-type and *rde-3* mutants (as described in Figure 2).
(H) Endogenous *oma-1*-associated CSR-1/22G is not required for RNAa.
Schematics and tabulations of RNAe and RNAa sensitivity are shown as described in Figures 3A and 3B.

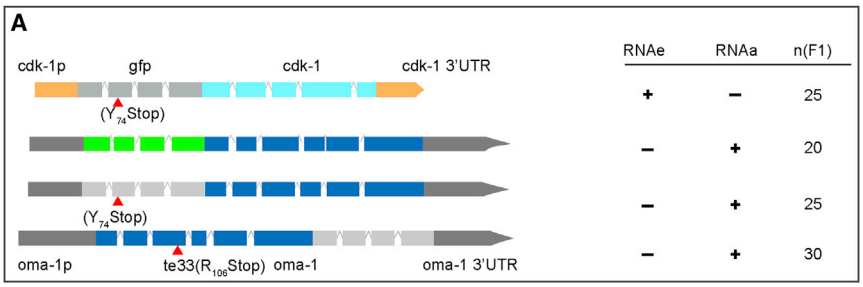

Figure 5. Premature Nonsense Mutations Do Not Prevent RNAa and RNAe

(A) Premature stop codons do not interfere with RNAa and RNAe activities. Schematics and tabulations of RNAe and RNAa sensitivity are shown as described in Figures 3A and 3B.
See also Figure S4.

gfp(Y_{74}stop)*::cdk-1* transgenes analyzed (n = 3) were able to potently induce silencing (n > 20, Figure 5A).

The *oma-1(te33)* mutation results in a premature stop (R_{106}stop) that was previously shown to be subject to suppression by NMD (Lin, 2003). We therefore introduced this mutation into an *oma-1::gfp* transgene and created single-copy transgenic strains. As expected, these strains failed to express detectable OMA-1::GFP protein (n = 3). When crossed to a silent *gfp::cdk-1* transgenic strain, this stop-codon-containing *oma-1* transgene was nevertheless proficient in activating the silent transgene (Figure 5A). Consistent with the idea that *oma-1*(R_{106}stop)*::gfp* is downregulated by NMD, we found that its mRNA expression was increased in NMD-defective *smg-5* mutant animals (Figure S4). Similarly, we found that transgenes engineered to contain Y_{74}stop within the *gfp* sequences of *gfp::oma-1*, although not expressed, could nevertheless transactivate a silent *gfp::cdk-1* transgene (Figure 5B). Thus, neither the RNAa nor RNAe pathways are sensitive to the inclusion of nonsense mutations within the ORFs of the inducing alleles, suggesting that these pathways scan mRNAs independently and likely upstream of the NMD pathway.

DISCUSSION

Regulation of mRNA Expression through the Entire Transcript

We have shown that piRNA targeting within the body of an mRNA inclusive of the ORF can modulate gene expression. The degree of silencing depends on opposing pathways that also act through the body of the mRNA to promote mRNA expression. piRNAs are abundantly expressed in the germlines of diverse animals (Aravin et al., 2006; Girard et al., 2006; Grivna et al., 2006; Lau et al., 2006; Ruby et al., 2006), and like miRNAs, piRNAs tolerate mismatched pairing (Ashe et al., 2012; Bagijn et al., 2012; Goh et al., 2015; Lee et al., 2012; Reuter et al., 2011; Shirayama et al., 2012) (Shen et al., 2018), further expanding their potential target space. Thus, the vast repertoire of piRNAs in metazoan germlines provides a wealth of potential post-transcriptional regulatory capacity. Our findings suggest that piRNAs can access and regulate mRNAs throughout the mature transcript, including the ORF, and that even the coding regions of mRNAs are free to sample regulatory inputs from piRNAs over evolutionary time. Moreover, because piRNAs are expressed as independent genes, they are also free to evolve independently, unconstrained by the coding requirements of their target regions. Thus, piRNAs may unlock a vast regulatory space, the coding regions of genes, for the control of gene expression.

How might the cell achieve mRNA regulation of the type observed here? One attractive model is suggested by the prominent localization of the Argonaute machinery (including PRG-1, CSR-1, and WAGO-1) within nuage (P granules) in the perinuclear zone (Batista et al., 2008; Claycomb et al., 2009; Gu et al., 2009). If nascent mRNAs are subject to scanning as they emerge from the nucleus prior to ribosome access, then the entire transcript including the ORF should be accessible to piRNA targeting. Increased piRNA targeting could reduce escape of the transcript and promote retention within a zone where WAGO 22G-RNA amplification occurs. Conversely, factors that promote escape from this regulatory zone will promote mRNA expression in *cis* (see model, Figure 6).

A paradox of the RNAa and RNAe systems is that RNAa, an activating mechanism, involves a cleavage-competent Argonaute, CSR-1, while RNAe, a silencing mechanism, involves several cleavage-incompetent Argonautes. WAGO Argonautes, unlike CSR-1, lack the conserved residues that coordinate Mg within their RNase H domains (Yigit et al., 2006). The key to this paradox is likely explained by the importance of amplification in the RNAe silencing mechanism. WAGO targeting leads to massive amplification of 22G-RNAs on WAGO targets, and only after 22G-RNA levels rise does silencing occur. 22G-RNA amplification is thought to occur within a subdomain of the P granule called the mutator focus (Phillips et al., 2012). By not cleaving their targets, WAGO Argonautes may ensure the preservation of the template RNAs needed to amplify and propagate the silencing signal. The paradox of CSR-1 as a protective, and yet cleavage-competent, Argonaute could in turn be explained if CSR-1 preferentially recognizes and cleaves the RdRP templates involved in WAGO-22G-RNA amplification, while avoiding the cleavage of the intact mRNAs corresponding to CSR-1 targets. This could explain how CSR-1 actively, and rapidly, disarms the silencing machinery when WAGOs become directed toward CSR-1 protected mRNA.

Balance and Tuning of Argonaute-Mediated Regulation

The above discussion suggests that Argonaute pathways are amplified and strongly transitive. But can they be balanced and tuned? In this study, we have explored transgene interactions in which the expression states of two complementary genes remain balanced, one OFF and one ON. This bimodal behavior suggests that the ultimate expression state of an mRNA is determined by mechanisms that sum activating and silencing signals, in *cis*, along the mRNA. For a gene that inherently resists piRNA silencing, we found that artificially increasing piRNA targeting led to reductions in expression that were stably inherited,

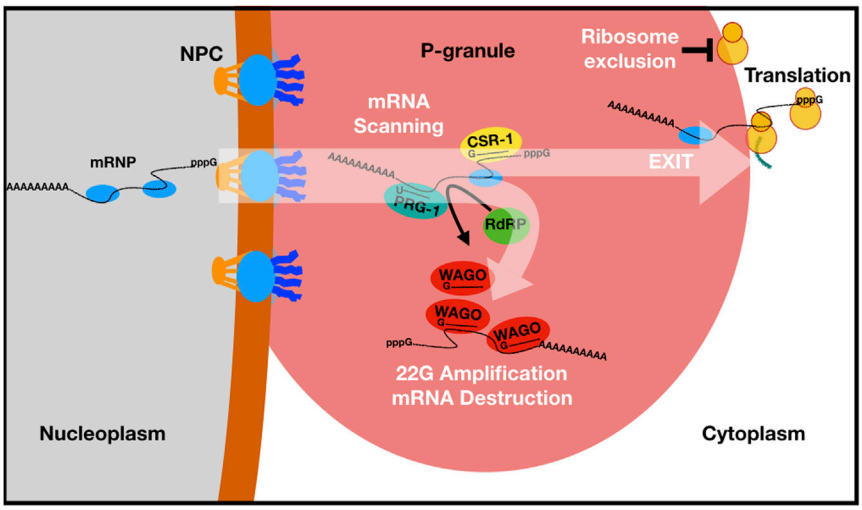

Figure 6. Model. piRNAs Scan mRNAs within Perinuclear Nuage prior to Translation Initiation

Schematic showing mRNPs exiting the nucleus through P granules. Binding factors and possibly covalent modification put in place during mRNA transcription and processing influence sensitivity to piRNA scanning. Three Argonaute systems within P granules are shown engaging the entire transcript including the ORF. The balance of positive and negative signals along an mRNA determines the fraction of molecules that escape destruction and gain access to the translation machinery.

demonstrating that piRNA can lower germline gene expression without completely silencing their targets. Importantly, the levels of WAGO or Piwi targeting are not the sole determinant of a gene's expression state. Rather, our findings also suggest that positive influences from unknown factors that act in *cis* on the mRNA sequences can override or partially counteract these silencing signals to preserve mRNA expression.

Our search for regions of a gene that confer resistance to silencing identified the ORF as necessary and sufficient. Analysis of these regions reveals no obvious features—e.g., absence of piRNA targeting or high levels of CSR-1 targeting—that could explain the reproducible ability of transgenes containing these sequences to activate silent transgenes. These findings suggest that, while CSR-1 mediates the transitive aspect of RNAa, other, as yet unknown features govern the inherent *cis*-acting resistance of the *oma-1* ORF to piRNA targeting, and presumably these still unknown features also underlie the ability of such transgenes to acquire or recruit CSR-1 targeting to their mRNA products.

Indeed, recent studies demonstrate that the entire germline transcriptome is under piRNA surveillance and that *C. elegans* piRNAs have physiologically important effects on the expression of at least one endogenous mRNA, *xol-1* (Shen et al., 2018; Tang et al., 2018). The *xol-1* mRNA behaves like the transgenes we describe here. We have shown that adding one new piRNA that targets *oma-1::gfp* reduced its expression but that adding three was necessary to drive complete silencing. Similarly, multiple piRNAs target *xol-1* cooperatively, inducing a large accumulation of WAGO 22G-RNAs (Shen et al., 2018). Moreover, *xol-1* silencing, like that of *oma-1::gfp*, requires continuous PRG-1 activity. Hundreds of other worm genes appear to be actively silenced by the piRNA pathway. Thus, future studies may identify additional physiologically important functions to the regulatory mechanisms revealed in these transgene studies. In summary, our findings suggest a temporal aspect to Argonaute-mediated regulation (likely prior to mRNA translation) and support the notion that *C. elegans* germline mRNAs, inclusive of their coding regions, undergo a period of comprehensive piRNA scanning during mRNA transit through perinuclear nuage.

EXPERIMENTAL PROCEDURES

Strains and Genetics

The *C. elegans* strains used in this study (Table S1) were derived from the Bristol N2 strain and cultured as described (Brenner, 1974). Transgenic strains were made using the MosSCI heat shock protocol combined with ivermectin selection as described (Frøkjær-Jensen et al., 2014; Shirayama et al., 2012).

Generation of Transgenic Strains by CRISPR/CAS9

21ux-1(anti-gfp), *21uIV-11498(anti-oma1)*, *and 21uIV-2675(anti-oma1)* were generated by a co-CRISPR strategy using *unc-22* sgRNA as a co-injection marker to enrich CRISPR/CAS9-mediated genome editing events (Kim et al., 2014). The vector expressing *rol-6 (su1006)*, a dominant allele conferring a roller phenotype, was used as a co-injection marker.

Small RNA Cloning and Deep Sequencing

Total RNA was extracted from adult worms using Trizol (Molecular Research Center). Small RNAs were further enriched using MirVana Kit (Thermo Fisher Scientific). Samples from wild-type and mutant were pretreated with a homemade 5′ polyphosphatase and were ligated to the 3′ adaptor linker 1 (5′ rAppAGATCGGAAGAGCACACGTCTGAACTCCAGTCA/3ddC/3′, IDT) using T4 RNA ligase 2 (M0351S, NEB). Subsequently, the 5′ adaptor (rArCrA rCrUrCrUrUrUrCrCrCrUrArCrArCrGrArCrGrCrUrCrUrUrCrCrGrArUrCrU) was ligated using T4 RNA ligase 1 (M0204S, NEB). The ligated products were converted to cDNA using SuperScript III (Thermo Fisher Scientific). Libraries were amplified by PCR and sequenced using the HiSeq or Miseq systems (Illumina) at the UMass Medical School Deep Sequencing facility.

Data Analysis

Small RNA sequencing results were analyzed using an established pipeline (Gu et al., 2012). Briefly, sequencing reads were sorted according to barcode sequences, and both 5′ and 3′ adaptor sequences were removed using a custom Perl script. Reads starting with G and 21 to 23 nt in length were mapped to WormBase WS215 allowing at most two mismatches and normalized to non-structural RNA reads. To account for differences in sequencing depth among samples, each read was normalized to total number of reads. Normalized counts were visualized in the UCSC genome browser. All scripts are available upon request.

Quantitative RT-PCR

The reverse transcription (RT) was performed using randomized primers by SuperScript III (Thermo Fisher Scientific). RT reaction was conducted in triplicate reactions. Real-time PCR was performed using SYBR Green PCR Master Mix (Applied Biosystems). Gene-specific primers were used to amplify *gfp* transcript. These transcripts were normalized to primers specific to *csr-1* transcripts. All statistical analysis was performed in Microsoft Excel. Error bars in the graph represent the standard deviation (SD).

Western Blotting Analysis

Cell lysate was prepared from synchronized population of L4 larvae and gravid adults. 50 μg lysate was loaded onto the precast polyacrylamide gel (Thermo Fisher Scientific), subjected to electrophoresis, and transferred onto the polyvinylidene difluoride membrane (Bio-Rad) with Trans-Blot Turbo Transfer System (Bio-Rad). The primary antibodies used were polyclonal anti-GLH-4 and polyclonal rabbit anti-GFP (GenScript, A01704). The secondary antibody is goat-anti-rabbit HRP (Abcam).

Imaging and Microscopy

Transgenic worms expressing GFP were mounted on RITE-ON glass slides (Beckton Dickinson) in the presence of 0.2 mM levamisole. Epi-fluorescence and differential interference contrast (DIC) microscopy were performed using an Axioplan2 Microscope (Zeiss). Images were processed using Axiovision software (Zeiss).

DATA AND SOFTWARE AVAILABILITY

The accession number for the small RNA data generated in this paper is NCBI: SRP108932.

SUPPLEMENTAL INFORMATION

Supplemental Information includes four figures, Supplemental Experimental Procedures, and one table and can be found with this article online at https://doi.org/10.1016/j.celrep.2018.02.009.

ACKNOWLEDGMENTS

We thank members of the Mello and Ambros labs for discussions and suggestions; D. Conte Jr. for critical review of the manuscript; W. Gu for providing the reagents for library preparation and the technical support; S. Vergara for technical support on northern blot; and E. Kittler and the UMass Deep Sequencing Core for Illumina sequencing. Some of the strains were provided by the Caenorhabditis Genetics Center supported by the NIH (P40 OD010440). W.T. is supported by the Hope Funds for Cancer Research Postdoctoral Fellowship (HFCR-15-06-03) and the NIH Pathway to Independence Award (GM124460). H.-C.L. is supported by the NIH Pathway to Independence Award (GM108866). The work was supported by a Hughes Medical Institute International Student Research Fellowship (G59107986) to M. Seth and NIH grants HD078253 to Z.W. and GM058800 and HD078253 to C.C.M. C.C.M. is a Howard Hughes Medical Institute Investigator.

AUTHOR CONTRIBUTIONS

Conceptualization, M. Seth, M. Shirayama, and C.C.M.; Methodology, M. Seth, M. Shirayama, and C.C.M.; Investigation, M. Seth, M. Shirayama, W.T., E.-Z.S., S.T., H.-C.L., and C.C.M.; Writing – Original Draft, M. Seth and C.C.M.; Review & Editing, M. Seth, W.T., and C.C.M.; Resources, M. Seth, M. Shirayama, and C.C.M.; Funding Acquisition, M. Seth, W.T., H.-C.L., Z.W., and C.C.M.; Supervision, Z.W. and C.C.M.

DECLARATION OF INTERESTS

The authors declare no competing interests.

Received: September 11, 2017
Revised: January 26, 2018
Accepted: February 1, 2018
Published: February 15, 2018

REFERENCES

Aravin, A., Gaidatzis, D., Pfeffer, S., Lagos-Quintana, M., Landgraf, P., Iovino, N., Morris, P., Brownstein, M.J., Kuramochi-Miyagawa, S., Nakano, T., et al. (2006). A novel class of small RNAs bind to MILI protein in mouse testes. Nature *442*, 203–207.

Ashe, A., Sapetschnig, A., Weick, E.M., Mitchell, J., Bagijn, M.P., Cording, A.C., Doebley, A.L., Goldstein, L.D., Lehrbach, N.J., Le Pen, J., et al. (2012). piRNAs can trigger a multigenerational epigenetic memory in the germline of C. elegans. Cell *150*, 88–99.

Bagijn, M.P., Goldstein, L.D., Sapetschnig, A., Weick, E.M., Bouasker, S., Lehrbach, N.J., Simard, M.J., and Miska, E.A. (2012). Function, targets, and evolution of *Caenorhabditis elegans* piRNAs. Science *337*, 574–578.

Baker, K.E., and Parker, R. (2004). Nonsense-mediated mRNA decay: terminating erroneous gene expression. Curr. Opin. Cell Biol. *16*, 293–299.

Batista, P.J., Ruby, J.G., Claycomb, J.M., Chiang, R., Fahlgren, N., Kasschau, K.D., Chaves, D.A., Gu, W., Vasale, J.J., Duan, S., et al. (2008). PRG-1 and 21U-RNAs interact to form the piRNA complex required for fertility in C. elegans. Mol. Cell *31*, 67–78.

Bhaya, D., Davison, M., and Barrangou, R. (2011). CRISPR-Cas systems in bacteria and archaea: versatile small RNAs for adaptive defense and regulation. Annu. Rev. Genet. *45*, 273–297.

Brenner, S. (1974). The genetics of *Caenorhabditis elegans*. Genetics *77*, 71–94.

Chang, Y.F., Imam, J.S., and Wilkinson, M.F. (2007). The nonsense-mediated decay RNA surveillance pathway. Annu. Rev. Biochem. *76*, 51–74.

Claycomb, J.M., Batista, P.J., Pang, K.M., Gu, W., Vasale, J.J., van Wolfswinkel, J.C., Chaves, D.A., Shirayama, M., Mitani, S., Ketting, R.F., et al. (2009). The Argonaute CSR-1 and its 22G-RNA cofactors are required for holocentric chromosome segregation. Cell *139*, 123–134.

Conine, C.C., Batista, P.J., Gu, W., Claycomb, J.M., Chaves, D.A., Shirayama, M., and Mello, C.C. (2010). Argonautes ALG-3 and ALG-4 are required for spermatogenesis-specific 26G-RNAs and thermotolerant sperm in *Caenorhabditis elegans*. Proc. Natl. Acad. Sci. USA *107*, 3588–3593.

Conine, C.C., Moresco, J.J., Gu, W., Shirayama, M., Conte, D., Jr., Yates, J.R., 3rd, and Mello, C.C. (2013). Argonautes promote male fertility and provide a paternal memory of germline gene expression in *C. elegans*. Cell *155*, 1532–1544.

Cox, D.N., Chao, A., Baker, J., Chang, L., Qiao, D., and Lin, H. (1998). A novel class of evolutionarily conserved genes defined by piwi are essential for stem cell self-renewal. Genes Dev. *12*, 3715–3727.

Dickinson, D.J., and Goldstein, B. (2016). CRISPR-based methods for *Caenorhabditis elegans* genome engineering. Genetics *202*, 885–901.

Fire, A., Xu, S., Montgomery, M.K., Kostas, S.A., Driver, S.E., and Mello, C.C. (1998). Potent and specific genetic interference by double-stranded RNA in *Caenorhabditis elegans*. Nature *391*, 806–811.

Friedland, A.E., Tzur, Y.B., Esvelt, K.M., Colaiácovo, M.P., Church, G.M., and Calarco, J.A. (2013). Heritable genome editing in *C. elegans* via a CRISPR-Cas9 system. Nat. Methods *10*, 741–743.

Frøkjær-Jensen, C., Davis, M.W., Sarov, M., Taylor, J., Flibotte, S., LaBella, M., Pozniakovsky, A., Moerman, D.G., and Jorgensen, E.M. (2014). Random and targeted transgene insertion in *Caenorhabditis elegans* using a modified Mos1 transposon. Nat. Methods *11*, 529–534.

Gerson-Gurwitz, A., Wang, S., Sathe, S., Green, R., Yeo, G.W., Oegema, K., and Desai, A. (2016). A small RNA-catalytic Argonaute pathway tunes germline transcript levels to ensure embryonic divisions. Cell *165*, 396–409.

Ghildiyal, M., and Zamore, P.D. (2009). Small silencing RNAs: an expanding universe. Nat. Rev. Genet. *10*, 94–108.

Girard, A., Sachidanandam, R., Hannon, G.J., and Carmell, M.A. (2006). A germline-specific class of small RNAs binds mammalian Piwi proteins. Nature *442*, 199–202.

Goh, W.S., Falciatori, I., Tam, O.H., Burgess, R., Meikar, O., Kotaja, N., Hammell, M., and Hannon, G.J. (2015). piRNA-directed cleavage of meiotic transcripts regulates spermatogenesis. Genes Dev. *29*, 1032–1044.

Gou, L.T., Dai, P., Yang, J.H., Xue, Y., Hu, Y.P., Zhou, Y., Kang, J.Y., Wang, X., Li, H., Hua, M.M., et al. (2014). Pachytene piRNAs instruct massive mRNA elimination during late spermiogenesis. Cell Res. *24*, 680–700.

Grimson, A., Farh, K.K., Johnston, W.K., Garrett-Engele, P., Lim, L.P., and Bartel, D.P. (2007). MicroRNA targeting specificity in mammals: determinants beyond seed pairing. Mol. Cell *27*, 91–105.

Grivna, S.T., Beyret, E., Wang, Z., and Lin, H. (2006). A novel class of small RNAs in mouse spermatogenic cells. Genes Dev. *20*, 1709–1714.

Gu, W., Shirayama, M., Conte, D., Jr., Vasale, J., Batista, P.J., Claycomb, J.M., Moresco, J.J., Youngman, E.M., Keys, J., Stoltz, M.J., et al. (2009). Distinct argonaute-mediated 22G-RNA pathways direct genome surveillance in the *C. elegans* germline. Mol. Cell *36*, 231–244.

Gu, W., Lee, H.C., Chaves, D., Youngman, E.M., Pazour, G.J., Conte, D., Jr., and Mello, C.C. (2012). CapSeq and CIP-TAP identify Pol II start sites and reveal capped small RNAs as *C. elegans* piRNA precursors. Cell *151*, 1488–1500.

Helwak, A., Kudla, G., Dudnakova, T., and Tollervey, D. (2013). Mapping the human miRNA interactome by CLASH reveals frequent noncanonical binding. Cell *153*, 654–665.

Ipsaro, J.J., Haase, A.D., Knott, S.R., Joshua-Tor, L., and Hannon, G.J. (2012). The structural biochemistry of Zucchini implicates it as a nuclease in piRNA biogenesis. Nature *491*, 279–283.

Izumi, N., Shoji, K., Sakaguchi, Y., Honda, S., Kirino, Y., Suzuki, T., Katsuma, S., and Tomari, Y. (2016). Identification and functional analysis of the pre-piRNA 3′ trimmer in silkworms. Cell *164*, 962–973.

Jinek, M., East, A., Cheng, A., Lin, S., Ma, E., and Doudna, J. (2013). RNA-programmed genome editing in human cells. eLife *2*, e00471.

Kim, H., Ishidate, T., Ghanta, K.S., Seth, M., Conte, D., Jr., Shirayama, M., and Mello, C.C. (2014). A co-CRISPR strategy for efficient genome editing in *Caenorhabditis elegans*. Genetics *197*, 1069–1080.

Lau, N.C., Seto, A.G., Kim, J., Kuramochi-Miyagawa, S., Nakano, T., Bartel, D.P., and Kingston, R.E. (2006). Characterization of the piRNA complex from rat testes. Science *313*, 363–367.

Lee, R.C., Feinbaum, R.L., and Ambros, V. (1993). The *C. elegans* heterochronic gene lin-4 encodes small RNAs with antisense complementarity to lin-14. Cell *75*, 843–854.

Lee, H.C., Gu, W., Shirayama, M., Youngman, E., Conte, D., Jr., and Mello, C.C. (2012). *C. elegans* piRNAs mediate the genome-wide surveillance of germline transcripts. Cell *150*, 78–87.

Lewis, B.P., Burge, C.B., and Bartel, D.P. (2005). Conserved seed pairing, often flanked by adenosines, indicates that thousands of human genes are microRNA targets. Cell *120*, 15–20.

Lin, R. (2003). A gain-of-function mutation in oma-1, a *C. elegans* gene required for oocyte maturation, results in delayed degradation of maternal proteins and embryonic lethality. Dev. Biol. *258*, 226–239.

Lin, H., and Spradling, A.C. (1997). A novel group of pumilio mutations affects the asymmetric division of germline stem cells in the *Drosophila* ovary. Development *124*, 2463–2476.

Marraffini, L.A., and Sontheimer, E.J. (2010). CRISPR interference: RNA-directed adaptive immunity in bacteria and archaea. Nat. Rev. Genet. *11*, 181–190.

Nishimasu, H., Ishizu, H., Saito, K., Fukuhara, S., Kamatani, M.K., Bonnefond, L., Matsumoto, N., Nishizawa, T., Nakanaga, K., Aoki, J., et al. (2012). Structure and function of Zucchini endoribonuclease in piRNA biogenesis. Nature *491*, 284–287.

Phillips, C.M., Montgomery, T.A., Breen, P.C., and Ruvkun, G. (2012). MUT-16 promotes formation of perinuclear mutator foci required for RNA silencing in the C. elegans germline. Genes Dev. *26*, 1433–1444.

Presnyak, V., Alhusaini, N., Chen, Y.H., Martin, S., Morris, N., Kline, N., Olson, S., Weinberg, D., Baker, K.E., Graveley, B.R., and Coller, J. (2015). Codon optimality is a major determinant of mRNA stability. Cell *160*, 1111–1124.

Reuter, M., Berninger, P., Chuma, S., Shah, H., Hosokawa, M., Funaya, C., Antony, C., Sachidanandam, R., and Pillai, R.S. (2011). Miwi catalysis is required for piRNA amplification-independent LINE1 transposon silencing. Nature *480*, 264–267.

Ruby, J.G., Jan, C., Player, C., Axtell, M.J., Lee, W., Nusbaum, C., Ge, H., and Bartel, D.P. (2006). Large-scale sequencing reveals 21U-RNAs and additional microRNAs and endogenous siRNAs in *C. elegans*. Cell *127*, 1193–1207.

Schisa, J.A., Pitt, J.N., and Priess, J.R. (2001). Analysis of RNA associated with P granules in germ cells of *C. elegans* adults. Development *128*, 1287–1298.

Seth, M., Shirayama, M., Gu, W., Ishidate, T., Conte, D., Jr., and Mello, C.C. (2013). The *C. elegans* CSR-1 argonaute pathway counteracts epigenetic silencing to promote germline gene expression. Dev. Cell *27*, 656–663.

Shen, E.-Z., Chen, H., Ozturk, A.R., Tu, S., Shirayama, M., Tang, W., Ding, Y.-H., Dai, S.-Y., Weng, Z., and Mello, C.C. (2018). Identification of piRNA binding sites reveals the Argonaute regulatory landscape of the *C. elegans* germline. Cell, Published online February 15, 2018. https://doi.org/10.1016/j.cell.2018.02.002.

Sheth, U., Pitt, J., Dennis, S., and Priess, J.R. (2010). Perinuclear P granules are the principal sites of mRNA export in adult *C. elegans* germ cells. Development *137*, 1305–1314.

Shirayama, M., Seth, M., Lee, H.C., Gu, W., Ishidate, T., Conte, D., Jr., and Mello, C.C. (2012). piRNAs initiate an epigenetic memory of nonself RNA in the *C. elegans* germline. Cell *150*, 65–77.

Tang, W., Tu, S., Lee, H.C., Weng, Z., and Mello, C.C. (2016). The RNase PARN-1 trims piRNA 3′ ends to promote transcriptome surveillance in *C. elegans*. Cell *164*, 974–984.

Tang, W., Seth, M., Tu, S., Shen, E.-Z., Li, Q., Shirayama, M., Weng, Z., and Mello, C.C. (2018). A sex chromosome piRNA promotes robust dosage compensation and sex determination in *C. elegans*. Dev. Cell *44*, Published online February 15, 2018. https://doi.org/10.1016/j.devcel.2018.01.025.

Updike, D.L., and Strome, S. (2009). A genomewide RNAi screen for genes that affect the stability, distribution and function of P granules in *Caenorhabditis elegans*. Genetics *183*, 1397–1419.

Updike, D., and Strome, S. (2010). P granule assembly and function in *Caenorhabditis elegans* germ cells. J. Androl. *31*, 53–60.

Updike, D.L., Hachey, S.J., Kreher, J., and Strome, S. (2011). P granules extend the nuclear pore complex environment in the *C. elegans* germ line. J. Cell Biol. *192*, 939–948.

Vourekas, A., Zheng, Q., Alexiou, P., Maragkakis, M., Kirino, Y., Gregory, B.D., and Mourelatos, Z. (2012). Mili and Miwi target RNA repertoire reveals piRNA biogenesis and function of Miwi in spermiogenesis. Nat. Struct. Mol. Biol. *19*, 773–781.

Wedeles, C.J., Wu, M.Z., and Claycomb, J.M. (2013). Protection of germline gene expression by the *C. elegans* Argonaute CSR-1. Dev. Cell *27*, 664–671.

Wightman, B., Ha, I., and Ruvkun, G. (1993). Posttranscriptional regulation of the heterochronic gene lin-14 by lin-4 mediates temporal pattern formation in *C. elegans*. Cell *75*, 855–862.

Yigit, E., Batista, P.J., Bei, Y., Pang, K.M., Chen, C.C., Tolia, N.H., Joshua-Tor, L., Mitani, S., Simard, M.J., and Mello, C.C. (2006). Analysis of the *C. elegans* Argonaute family reveals that distinct Argonautes act sequentially during RNAi. Cell *127*, 747–757.

Cell Reports, Volume *22*

Supplemental Information

The Coding Regions of Germline mRNAs Confer Sensitivity to Argonaute Regulation in *C. elegans*

Meetu Seth, Masaki Shirayama, Wen Tang, En-Zhi Shen, Shikui Tu, Heng-Chi Lee, Zhiping Weng, and Craig C. Mello

SUPPLEMENTAL FIGURES

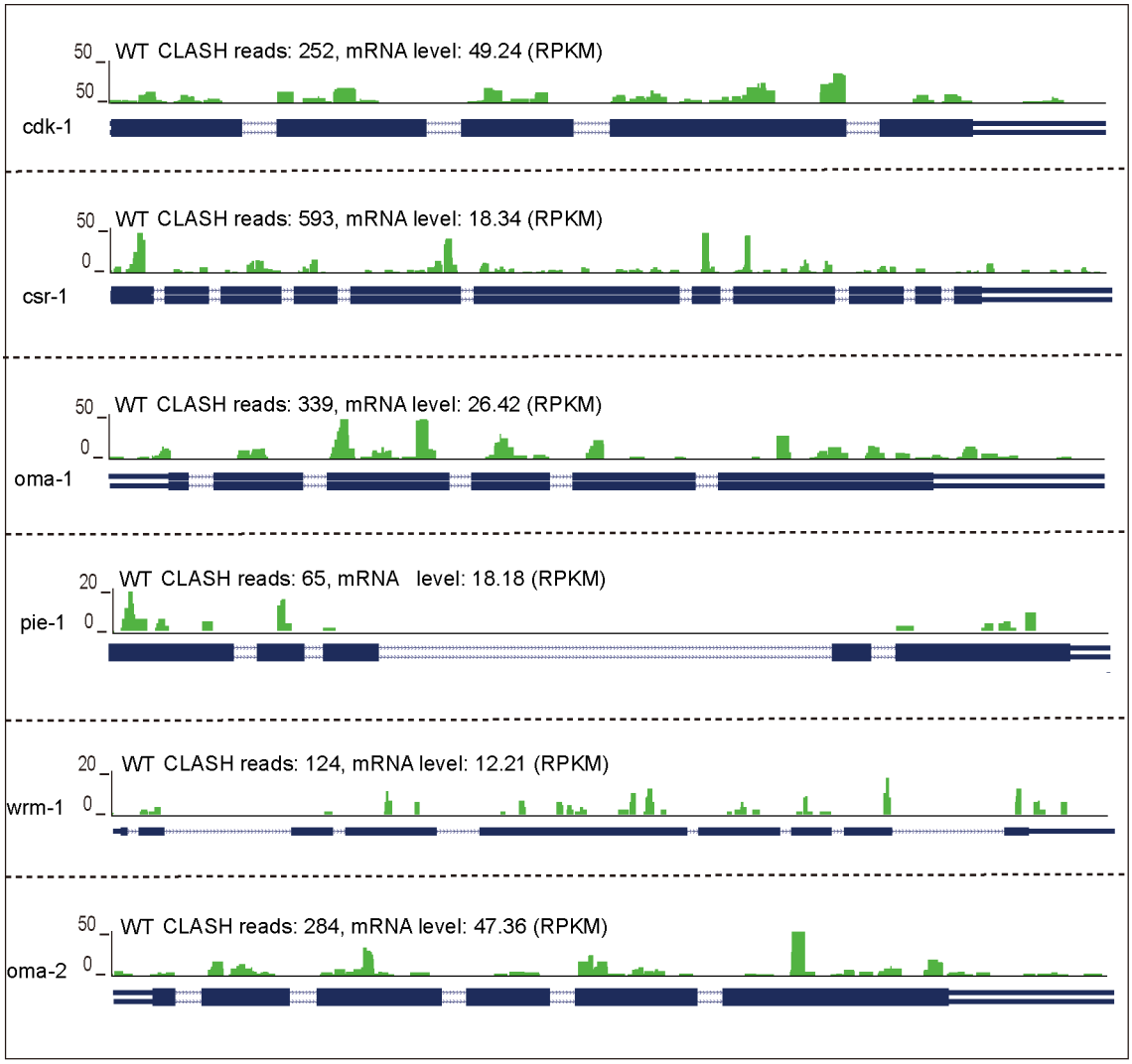

Figure S1. piRNAs target germline-expressed mRNAs associated with RNAe and RNAa. ***Related to Figures 1 and 2.***

Genome browser views illustrating the distributions of piRNA target sites along the genes *cdk-1*, *csr-1*, *oma-1*, *pie-1*, *wrm-1*, and *oma-2*. These piRNA target sites were identified by CLASH (Shen et al., 2018). y-axis indicates the number of CLASH reads.

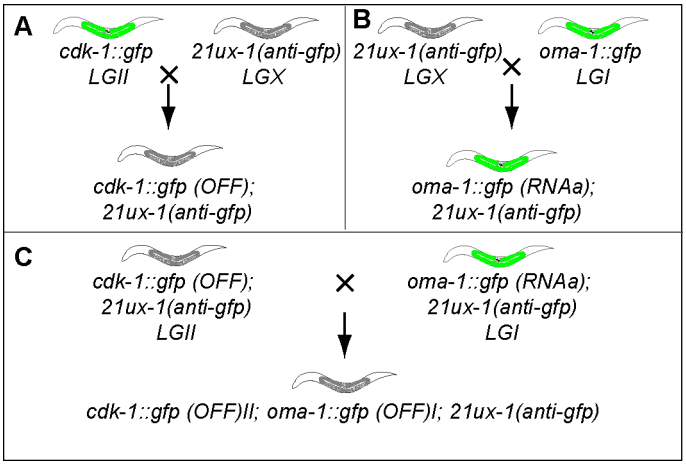

Figure S2. Transgenes differ in their sensitivity to piRNA targeting. ***Related to Figure 2***
(A-C) Cartoon of worms illustrating crosses between different transgenic strains. The cartoon indicates whether the transgene is ON (green) or OFF (grey).

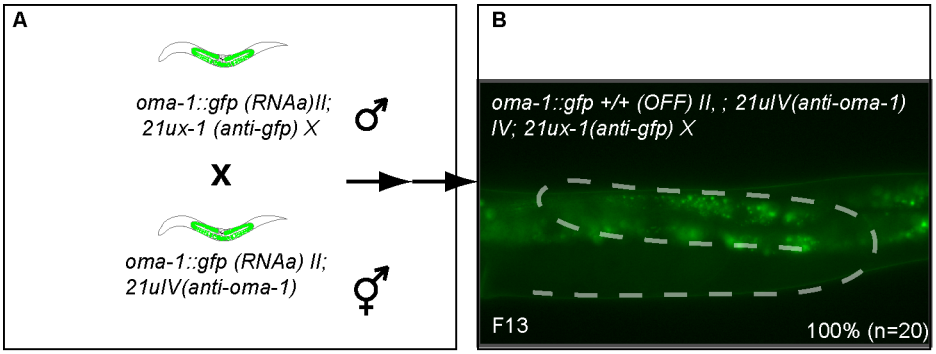

Figure S3. Increasing piRNA targeting induces *oma-1::gfp* to silence. *Related to Figure 3*
(A) Cartoon of worms representing the expression of *oma-1::gfp* by the individual piRNA (*21ux-1-anti-gfp*) targeting either GFP or *oma-1 (21uIV-antioma-1*) targeting *oma-1*.
(B) Silencing of *Oma-1::gfp* transgene by three different piRNAs.

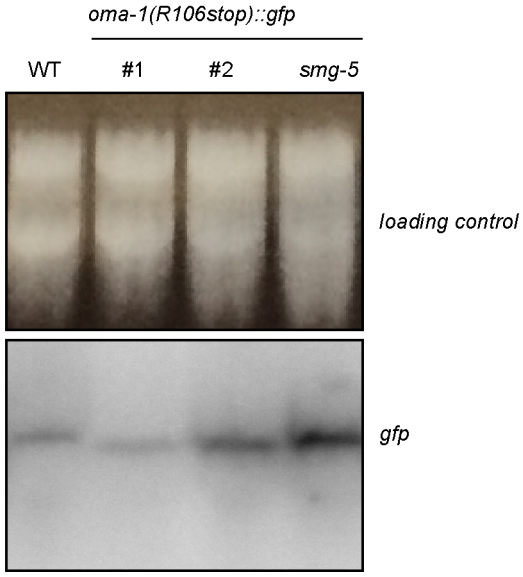

Figure S4. Increase in mRNA expression in the *smg-5* mutant by Northern Blot. ***Related to Figure 5***
Northern blot analysis of *oma-1::gfp*-RNA using *gfp* probe (168-nt from the first exon of *gfp*). Total RNA was prepared from two different transgenic strains (#1 and #2, as indicated). 20 µg total RNA was loaded per lane.

SUPPLEMENTAL EXPERIMENTAL PROCEDURES, Related to Figures 1, 2, and 3.

MosSCI strain constructs

oma-1: A SpeI–AleI fragment containing *oma-1::gfp* was excised from pRL475 (gift from R. Lin) and inserted into plasmid B1496, a modified version of the LGII MosSCI targeting vector pCFJ151 to obtain targeting plasmid M1001 (Seth et al., 2013). M1001 was further modified to make various constructs of *oma-1*. Detailed description is available on request. A DNA mixture containing 50 ng/µl of modified plasmid M1001 was injected into WM186, and a modified MosSCI heat shock method (Shirayama et al., 2012) was used to generate the single-copy insertion line WM288.
For direct injection, a DNA mixture containing 10 ng/µl of modified plasmid M1001 was injected into EG4322, and the direct insertion method MosSCI (Frokjaer-Jensen et al., 2008; Shirayama et al., 2012) was used to generate the single-copy insertion line.

CRISPR method

21ux-1(anti-gfp), *21uIV-11498 (anti-oma1) and 21uIV-2675 (anti-oma1)* was generated by a co-CRISPR strategy using *unc-22* sgRNA as a co-injection marker to enrich CRISPR/CAS9-mediated genome editing events (Kim et al., 2014). The vector expressing *rol-6 (su1006)*, a dominant allele conferring a roller phenotype, was used as a co-injection marker.

Table S1. [*C. elegans* Strains used in this study], Related to Figures 1, 3, 4 and 5

Strain	Genotype	Method
EG4322	Mos1(ttTi5605) II; unc-119(ed9) III	
EG6701	Mos1(ttTi4348) II; unc-119(ed9) III	
WM186	avr-14(ad1302) I; Mos1(ttTi5605) II; unc-119 (ed9) III; glc-1(pk54::Tc1) avr-15(ad1051) V	
WM572	avr-14(ad1302) I; Mos1(ttTi4348) II; unc-119 (ed9) III; glc-1(pk54::Tc1) avr-15(ad1051) V	Cross
WM240	neSi10 [gfp::csr-1(RNAe), cb-unc-119(+)] IV; unc-119(ed9) III	MosSCI
WM573	neSi22 [oma-1::gfp (RNAa), cb-unc-119(+)] II; neSi10 [gfp::csr-1(RNAe), cb-unc-119(+)] IV (RNAe); unc-119(ed9) III	Cross
WM574	prg-1(tm872) I; neSi22 [oma-1::gfp (RNAa), cb-unc-119(+)] II; neSi10 [gfp::csr-1(RNAe), cb-unc-119(+)] IV; unc-119(ed9) III	Cross
WM242	neSi12 [cdk-1::gfp(+), cb-unc-119(+)] II; unc-119(ed9) III.	MosSCI
WM575	[21ux-1 (anti-gfp) (ne4561)] X	CRISPR
WM576	neSi12 [cdk-1::gfp(+), cb-unc-119(+)] II; unc-119(ed9) III; 21ux-1 (anti-gfp) (ne4561) X	Cross
WM577	neSi32 [oma-1::gfp, (cb-unc-119+)] I; avr-14(ad1302) I; unc-119 (ed9) III; glc-1(pk54::Tc1) avr-15(ad1051) V]; [21ux-1 (anti-gfp) (ne4561)] X	MosSCI
WM578	neSi22 [oma-1::gfp, (cb-unc-119+)] I; neSi12 [cdk-1::gfp (RNAe), cb-unc-119(+)] II; unc-119 (ed9) III; [21ux-1 (anti-gfp) (ne4561)] X	Cross
WM288	neSi22 [oma-1::gfp (RNAa), cb-unc-119(+)] II; oma-1 (ne4562) (complete del) IV	MosSCI
WM593	neSi22 [oma-1::gfp (RNAa), cb-unc-119(+)] II; oma-1 (ne4562) (complete del) IV; [21ux-1 (anti-gfp) (ne4561)] X	Cross
WM579	neSi33 [oma-1::gfp, cb-unc-119(+)] I; unc-119 (ed9) III; [21uIV-2675 (anti-oma-1), 21uIV-11498 (anti-oma-1) (ne4562)] IV, #64	CRISPR
WM580	neSi33 [oma-1::gfp, cb-unc-119(+)] I; unc-119 (ed9) III; [21uIV-2675 (anti-oma-1), 21uIV-11498 (anti-oma-1) (ne4562)] IV; [21ux-1 (anti-gfp) (ne4561)] X	Cross
WM581	neSi34 [cdk-1p::oma-1::gfp::cdk-1 3'UTR, cb-unc-119(+)] II; unc-119(ed9)III	MosSCI
WM582	neSi35 [oma-1p::gfp:cdk-1:: oma-1 3'UTR, cb-unc-119(+)] II; unc-119(ed9)III	MosSCI

WM583	neSi36 [oma-1p::cdk-1:gfp:: oma-1 3'UTR, cb-unc-119(+)] II; unc-119(ed9)III	MosSCI
WM584	neSi37 [oma-1::gfp (cDNA), cb-unc-119(+)] II; unc-119(ed9)III; oma-1 (ne4562) (complete del) IV	MosSCI
WM585	neSi38 [codon altered oma-1::gfp, cb-unc-119(+)] II; avr-14(ad1302) I; unc-119(ed9) III, oma-1 (ne4562) (complete del) IV, avr-15(ad1051)glc1 V	MosSCI
WM586	(rde-3) (ne4563) I; avr-14(ad1302) I; [codon altered oma-1::gfp, (cb-unc-119(+)] II; unc-119(ed9) III, oma-1 (ne4562) (complete del) IV , avr 15(ad1051)glc1V	CRISPR
WM587	avr-14 (ad1302) I; [oma-1::gfp, +1 Frame (cb-unc-119+)] II; unc-119(ed9) III, oma-1 (ne4562) (complete del) IV, avr-15(ad1051)glc1 V	MosSCI
WM588	neSi39 [oma-1::gfp, (cb-unc-119+)] II; unc-119(ed9) III, avr-14(ad1302) I; avr-15(ad1051)glc1 V; oma-1 (ne4562) (complete del) IV	MosSCI
WM589	neSi40 [gfp (Y74STOP)::cdk-1, (cb-unc-119+)] II; unc-119(ed9) III, avr-15(ad1051)glc1 V	MosSCI
WM590	neSi41 [gfp::oma-1, (cb-unc-119+)] II; avr-14(ad1302) I; unc-119(ed9) III, avr-15(ad1051)glc1 V; oma-1 (ne4562) (complete del) IV	MosSCI
WM591	neSi42 [gfp (Y74STOP)::oma-1, (cb-unc-119+)] II; avr-14(ad1302) I; unc-119(ed9) III, avr-15(ad1051)glc1 V; oma-1 (ne4562) (complete del) IV	MosSCI
WM592	neSi43 [oma-1::gfp te33(R106STOP), cb-unc-119(+)] II; avr-14(ad1302) I; unc-119(ed9) III, avr-15(ad1051)glc1 V	MosSCI

Table S2. Oligonucleotides. Related to Figure 2, 3 and 4

Oligo name	**Oligo sequence**
Real-time PCR	
*csr-1*_cmo17005_F	CTGCCCTTCTCCGTCACTTA
*csr-1*_cmo17006_F	TTGATGGCTCGTTGAACTTG
Oma-1::gfp_cmo17009_F	ATTGGCCGAAAATATGACCA
Oma-1::gfp_cmo17009_R	TCACCTTCACCCTCTCCACT
Northern Blots	
*gfp*_ cmo17007_F	AGTAAAGGAGAAGAACTTTT

*gfp*_cmo17008_R	CCATGGAACAGGTAGTTTTC